THE IMPORTANCE OF SURFACE PROPERTIES OF GRAPHITE DURING THE FIRST LITHIUM-INTERCALATION

Cathie Vix-Guterl, R. Gadiou, J. Dentzer, Institut de Chimie des Surfaces et Interfaces, 15 rue Jean Starcky , 68057 Mulhouse, France, cathie.vix@uha.fr
Petr Novák, Nicolas Tran, Hilmi Buqa, Paul Scherrer Institut, Electrochemistry Laboratory, CH - 5232 Villigen PSI, Switzerland
M. E. Spahr" H. Wilhelm, TIMCAL SA, CH-6743 Bodio TI, Switzerland

INTRODUCTION

Lithium-ion batteries are now the cell-of-choice to power portable electronic applications such as cellular phones, notebook computers, and camcorders. Recent worldwide interest in pure electric and hybrid vehicle has accelerated the research in laboratories and industry of larger-sized rechargeable lithium-ion batteries [1]. Their use in mobile applications requires especially to improve their energy density and consequently to reduce the irreversible capacity.
Graphitic carbon materials are nowadays favored as negative electrode in commercial lithium-ion batteries. During the first discharge of such a battery, a solid electrolyte interphase (SEI) is formed and acts as a passivation layer on the graphite grain surfaces. This layer is responsible for an irreversible capacity “loss” but also serves as protection against co-intercalation of solvent molecules into the graphite and exfoliation of the graphite surface [2]. Especially for the high crystalline graphite, the formation of this passivation layer is of prime importance since it suppresses any further electrolyte decomposition and particularly avoids electrochemical exfoliation of the structure [3,4,5]. A complete understanding of the formation process of this SEI layer with the identification of the critical parameters influencing its efficiency is essential and is a prerequisite for the development of improved graphite electrode materials for advanced lithium-ion batteries.
It is now well known that the composition of the SEI layer which results from electrolyte decomposition products depends on several parameters such as the graphite type, the electrolyte composition (nature of the salt, the solvent used) and the presence of electrolyte impurities [6,7,8]. The influence of the graphite characteristics has been already investigated [9,10,11]. We observed that the surface properties of a highly crystalline graphite material have a significant influence on the electrolyte decomposition and passivation mechanism during the first electrochemical lithium insertion and, thus, on the SEI layer formation and composition. Several parameters were identified as being responsible. Among them the surface groups chemistry and the amount of surface defects, both parameters being related [10,11]. Recently, we showed that the ASA concept is a very useful tool to predict the exfoliation tendency [10]. To confirm the influence of the ASA and thus the degree of structural order at the surface on the exfoliation tendency, graphite with different active surface area were prepared and electrochemically tested.

EXPERIMENTAL

The surface characteristics of the TIMREX® SLX50 can be easily modified after thermal modifications under various gas atmosphere without significantly changing the bulk properties (especially the total surface area) and the particle size distribution of the product. For this, the TIMREX® SLX50 graphite was heated at 1300°C under an argon flow and maintained 1 min or 1 hour, respectively, at this temperature. After the heat treatment, the graphite sample was either cooled in an argon atmosphere until room temperature or quenched in air. The air quenching causes a slight oxidation of the carbon sample. After cooling down to room temperature, the samples are exposed to the air atmosphere. The active surface area (ASA) was determined at 950°C under vacuum (10^{-4} Pa) by outgassing the sample in an elsewhere described experimental set-up at 950°C under vacuum (10^{-4} Pa) and following the procedure described elsewhere [12,13].
The electrochemical experiments were performed with a metallic lithium counter electrode in two-electrode arrangement in standard laboratory cells as described elsewhere [11]. The lithium foil (Aldrich) and 1 M $LiPF_6$ in EC:DMC [1:1] (Ferro) were used without any further treatment. Working electrodes were prepared by doctor-blading the SLX50 graphite (TIMCAL SA, Bodio, Switzerland) with polyvinylidene fluoride (SOLEF 1015, Solvay) binder onto a copper current collector. The electrodes were vacuum dried at 120°C and contained ca. 10 mg of graphite (their composition was 90 wt.% graphite and 10 wt.% PVDF). Galvanostatic measurements were performed at specific currents of 10 mA/g of carbon to complete the SEI formation in the first Li^+ insertion cycle. After a potential of 5 mV vs. Li/Li^+ was reached, the discharging was continued at this constant potential until the current dropped below 5 mA/g. The charging was performed at a constant specific

current of 10 mA/g until a cut-off potential of 1.5 V vs. Li/Li^+ was reached. All measurements were carried out at room temperature.

RESULTS AND DISCUSSION

The Temperature Programmed Desorption (TDP) curves of the different SLX50 samples after chemisorption of O_2 at 300°C showed that the formation of CO and CO_2 is completed below 900°C as shown in Figure 1 for the sample SLX50 treated in argon during 1 hour. This indicates that the total amount of oxygen complexes formed on the active sites during the oxygen chemisorption was totally removed during the TPD.

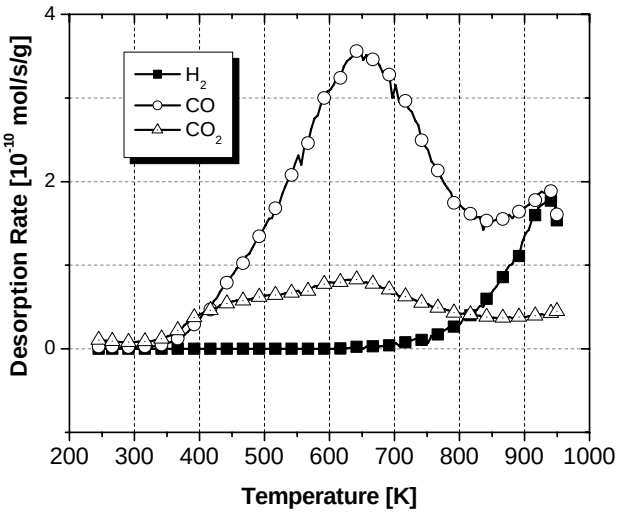

Fig. 1: Desorption rate of CO and CO_2 as a function of desorption temperature after oxygen chemisorption, for the "SLX50 1hr Ar" sample.

From the total amount of CO and CO_2 released after chemisorption, the ASA was calculated; the values obtained for the different SLX50 samples are reported in Table 1.

Graphite Sample	ASA m^2/g	Irrev. Cap. %; 1^{st} cycle
SLX50	0.30	8
SLX50 1hr. Ar	0.065	57
SLX50-1min. Ar	0.092	54
SLX50 1hr. Ar + air	0.44	10

Table 1: Active surface area (ASA) and irreversible capacity in the first cycle of graphite materials ("SLX50": as-received sample; "SLX50 1hr. Ar + air": as-received SLX50 sample treated 1 hour in an argon flow following by an air quenching for the cooling; "SLX50 1hr. Ar": as-received SLX50 sample treated 1 hour in an argon flow; "SLX50 1min. Ar": as-received SLX50 sample treated 1 min in an argon flow).

As expected, the heat treatment in argon has increased the structural ordering of the graphite and therefore removed surface defects, as indicating by the decrease of the ASA values. A subsequent air treatment leads to a mild oxidation of the graphite surface as pointed out by the increase of the ASA value after the argon treatment. For a detailed investigation of the film formation in the first cycle, we analyzed the irreversible charge "losses" and the galvanostatic charge curves of the first lithium insertion into the graphite. The charge "losses" (irreversible capacity, in %) of the graphite samples during the first cycle are indicated in Table 1. The curves of the first galvanostatic lithium intercalation into the graphite TIMREX® SLX50 and the three heat-treated SLX50 graphite samples are reported in Figure 2.

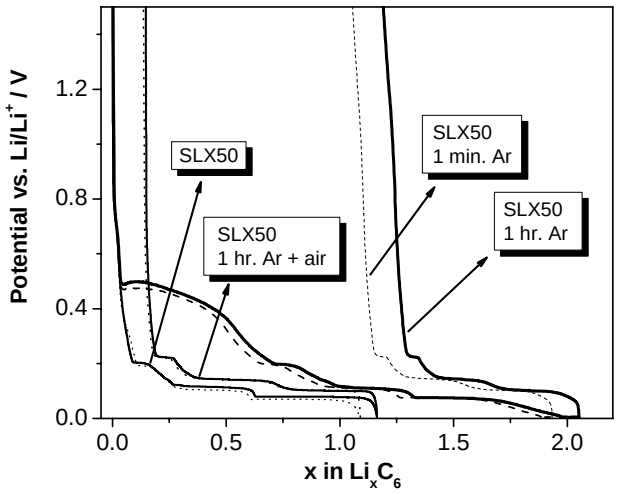

Fig. 2: First electrochemical lithium insertion into TIMREX® SLX50 (i) as received and (ii) heat treated at 1300°C in argon for 1 min and 1 h, respectively, and subsequently cooled down in argon and air atmosphere, respectively, in EC:DMC, 1M $LiPF_6$ electrolyte.

The pristine sample as well as the sample cooled down in air show the typical insertion properties expected for a highly crystalline graphite material. A reversible charge capacity (specific charge) of ca. 360 mAh/g could be observed at a specific current of 10 mA/g. No additional plateau is observed with these two samples suggesting that a protective passivation film (SEI) was formed on the graphite surface. This is confirmed by the low irreversible charge "loss" (Table 1) and the *post mortem* analyses by SEM images of the charged graphite electrodes taken from dismantled half-cells (not shown here). Both, the as-received SLX50 and the "SLX50 1hr Ar + air" graphite electrodes show an uniform and relatively dense film on the graphite particles. No exfoliation of the graphite can be observed. In contrast, the heat-treated SLX50 graphite samples cooled under Ar atmosphere show an additional irreversible charge-consuming process manifested by an additional potential plateau during the first electrochemical lithium insertion (Fig.2) which was identified as the exfoliation of the graphite. The said potential plateau corresponds to the irreversible, charge consuming film formation process on the graphite surface freshly created by the exfoliation process. This relatively low potential plateau is typical for exfoliation in an EC based electrolyte. As a consequence, this irreversible process of graphite exfoliation significantly increases the "loss" of the specific charge during the first electrochemical lithium insertion, as shown in Table 1.

The comparison of the electrochemical data with the graphite surface characteristics reveals that the electrochemical behavior of the graphite can be correlated to the structural modifications occurring during the treatments, as it will be discussed below.

The evolution of the ASA of the graphite leads to modifications of the galvanostatic curves and the irreversible charge loss. After heat treatment in argon, the decrease of the ASA induces an important increase in the irreversible charge "loss" which is characteristic for an exfoliation process, as confirmed by SEM observations. It is interesting to note that, when the graphite sample heat-treated in argon is again exposed to air to increase the ASA (and consequently to increase the amount of surface defects), the exfoliation phenomenon isn't observed anymore. This may be related to the surface reactivity against the electrolyte. In fact, the higher the amount of active surface sites at the graphite surface, the higher the graphite surface reactivity that can be expected. A graphite material with a low ASA value will thus show a low reactivity towards the electrolyte. As

a result, the kinetics of the passivation layer formation will be slow and the passivation process will be not completed before the electrochemical exfoliation starts.
In contrast, the graphite material with a lower structural ordering (high ASA value) shows a higher reactivity towards the electrolyte and, thus, the kinetics of the formation of the passivation layer (SEI) will be enhanced. In this condition, the formation of the SEI layer is completed prior to the onset of the exfoliation. This is in agreement with the fact that the kinetics of formation of the passivation layer is related to the ASA.

3. Conclusion

The stability of highly crystalline graphite materials toward exfoliation of the graphite structure during the first electrochemical lithium insertion in mixed EC/DMC electrolyte systems depends on the reactivity of the graphite particles toward the electrolyte decomposition. This reactivity is related to the surface properties of the graphite. We show here that the surface properties and especially the active sites of the highly crystalline graphite material have a significant influence on the electrolyte decomposition and passivation process during the first electrochemical lithium insertion and, thus, on the SEI layer formation.
The elimination of surface defects by heat treatment (decrease of the ASA) hinders the formation of the SEI film and consequently favors the exfoliation of graphite. On the contrary, the increase in the ASA results in faster electrolyte decomposition and subsequent graphite surface passivation at potentials which are more positive than the potential at which the electrochemical exfoliation of graphite can be observed.
It is interesting to note that the electrochemical performance of a graphite material can be strongly modified by changing the active surface area of the graphite. We also confirm through this work that the concept of active sites is a suitable tool to predict the passivation behavior of the graphite.

4. Acknowledgements

The authors wish to thank the Swiss State Secretariat for Education and Research for financial support under the framework of the European research project CAMELiA.

[1] T. Horiba, K. Hironaka, T. Matsumura, T. Kai, M. Koseki, and Y. Muranaka, J. Power Sources 119-121 (2003) 893.
[2] K. Guerin, A. Fevrier-Bouvier, S. Flandrois, M. Couzi, B. Simon, and P. Biensan, J. Electrochem. Soc. 146 (1999) 3660.
[3] M. Winter, J. O. Besenhard, M. E. Spahr, and P. Novák, Adv. Mater. 10 (1979) 725.
[4] M. Winter, P. Novák, and A. Monnier, J. Electrochem. Soc. 145 (1998) 428.
[5] J. O. Besenhard, M. Winter, J. Yang, and W. Biberacher, J. Power Sources 54 (1995) 228.
[6] W. S. Kim, D. W. Park, H. J. Jung, and Y. K. Choi, Bulletin of The Korean Chemical Society 27 (2006) 82
[7] H. Buqa, A. Wuersig, D. Goers, L. J. Hardwick, M. Holzapfel, P. Novák, F. Krumeich, and M. E. Spahr, J. Power Sources 146 (2005) 134.
[8] M. R. Wagner, J. H. Albering, K. C. Moeller, J. O. Besenhard, and M. Winter, Electrochem. Commun. 7 (2005) 947.
[9] F. Joho, B. Rykart, A. Blome, P. Novák, H. Wilhelm, M. E. Spahr, J. Power Sources 97-98 (2001) 78.
[10] M. E. Spahr, H. Buqa, A. Wuersig, D. Goers, L. J. Hardwick, P. Novák, F. Krumeich, J. Dentzer, and C. Vix-Guterl, J. Power Sources 153 (2006) 300.
[11] M. E. Spahr, H. Wilhelm, T. Palladino, N. Dupont-Pavlovsky, D. Goers, F. Joho, and P. Novák, J. Power Sources 119-121 (2003) 543.
[12] N. R. Laine, F. J. Vastola, and P. L. Walker Jr., J. Phys. Chem. 67 (1963) 2030.
[13] C. Vix-Guterl, P. Ehrburger, World of Carbon, P. Delhaes (Ed.), Vol.2, p. 188, Taylor and Francis, London and New York, 2003